OPEN ACCESS

KING'S College LONDON

King's Research Portal

DOI:
10.1016/j.reprotox.2018.06.010

Document Version
Peer reviewed version

Link to publication record in King's Research Portal

Citation for published version (APA):
Rasinger, J. D., Carroll, T. S., Maranghi, F., Tassinari, R., Moracci, G., Altieri, I., Mantovani, A., Lundebye, A-K., & Hogstrand, C. (2018). Low dose exposure to HBCD, CB-153 or TCDD induces histopathological and hormonal effects and changes in brain protein and gene expression in juvenile female BALB/c mice. *Reproductive Toxicology*. https://doi.org/10.1016/j.reprotox.2018.06.010

Citing this paper
Please note that where the full-text provided on King's Research Portal is the Author Accepted Manuscript or Post-Print version this may differ from the final Published version. If citing, it is advised that you check and use the publisher's definitive version for pagination, volume/issue, and date of publication details. And where the final published version is provided on the Research Portal, if citing you are again advised to check the publisher's website for any subsequent corrections.

General rights
Copyright and moral rights for the publications made accessible in the Research Portal are retained by the authors and/or other copyright owners and it is a condition of accessing publications that users recognize and abide by the legal requirements associated with these rights.

•Users may download and print one copy of any publication from the Research Portal for the purpose of private study or research.
•You may not further distribute the material or use it for any profit-making activity or commercial gain
•You may freely distribute the URL identifying the publication in the Research Portal

Take down policy
If you believe that this document breaches copyright please contact librarypure@kcl.ac.uk providing details, and we will remove access to the work immediately and investigate your claim.

Download date: 04. May. 2023

Accepted Manuscript

Title: Low dose exposure to HBCD, CB-153 or TCDD induces histopathological and hormonal effects and changes in brain protein and gene expression in juvenile female BALB/c mice

Authors: J.D. Rasinger, T.S. Carroll, F. Maranghi, R. Tassinari, G. Moracci, I. Altieri, A. Mantovani, A.-K. Lundebye, C. Hogstrand

PII: S0890-6238(18)30168-0
DOI: https://doi.org/10.1016/j.reprotox.2018.06.010
Reference: RTX 7685

To appear in: *Reproductive Toxicology*

Received date: 30-4-2018
Revised date: 7-6-2018
Accepted date: 18-6-2018

Please cite this article as: Rasinger JD, Carroll TS, Maranghi F, Tassinari R, Moracci G, Altieri I, Mantovani A, Lundebye A-K, Hogstrand C, Low dose exposure to HBCD, CB-153 or TCDD induces histopathological and hormonal effects and changes in brain protein and gene expression in juvenile female BALB/c mice, *Reproductive Toxicology* (2018), https://doi.org/10.1016/j.reprotox.2018.06.010

This is a PDF file of an unedited manuscript that has been accepted for publication. As a service to our customers we are providing this early version of the manuscript. The manuscript will undergo copyediting, typesetting, and review of the resulting proof before it is published in its final form. Please note that during the production process errors may be discovered which could affect the content, and all legal disclaimers that apply to the journal pertain.

ACCEPTED MANUSCRIPT

Low dose exposure to HBCD, CB-153 or TCDD induces histopathological and hormonal effects and changes in brain protein and gene expression in juvenile female BALB/c mice

Rasinger J.D.[1,2]*, Carroll T.S.[2], Maranghi F.3, Tassinari R.[3], Moracci G.[3], Altieri I.[3] Mantovani A.[3], Lundebye A.-K.[1], Hogstrand C.[2]*

[1] Institute of Marine Research, Bergen, Norway.
[2] Department of Nutritional Sciences, School of Life Course Sciences, King's College London, UK.
[3] Istituto Superiore di Sanità, Rome, Italy.

***** Correspondence: josef.rasinger@hi.no; christer.hogstrand@kcl.ac.uk

Graphical Abstract

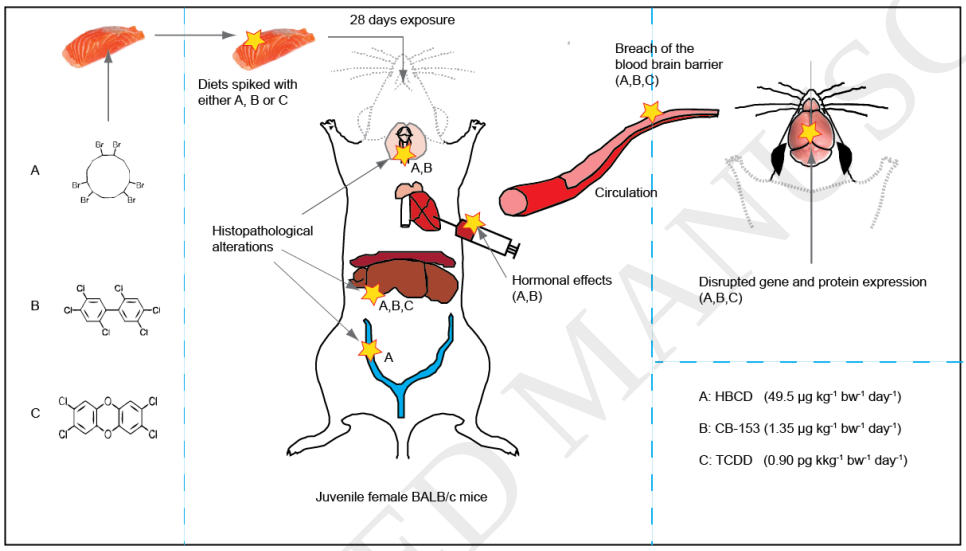

Highlights

- Toxicological relevant effects on post-natal development in female mice were observed after dietary exposure to HBCD, CB-153, or TCDD at doses below previously established effect levels
- Histopathological changes were found in liver (HBCD, CB-153, TCDD), thymus (HBCD, CB-153) and uterus (HBCD)
- HBCD, CB-153 and TCDD all caused alterations of protein and gene expression in the brain
- Effects on sex steroid signalling and serum levels were seen in response to HBCD or CB-153
- Genes involved in Ca2+ and Zn2+ signalling and in neurological disease were regulated by all three toxicants

ACCEPTED MANUSCRIPT

Abstract

Developmental health risks of chronical exposure to low doses of foodborne persistent organic pollutants (POP) are recognized but still largely uncharacterized. Juvenile female BALB/c mice exposed to either HBCD, CB-153 or TCDD at doses relevant to human dietary exposures (49.5 μg, 1.35 μg and 0.90 pg kg^{-1} bw^{-1} day^{-1} , respectively) for 28 days displayed histopathological changes in liver (HBCD, CB-153, TCDD), thymus (HBCD, CB-153) and uterus (HBCD), reduced serum oestradiol 17β (E2) levels (HBCD), increased serum testosterone (T) levels (CB-153) and an increased T/E2 ratio (HBCD). Proteomics analysis of brain provided molecular support for the HBCD-induced reduction in E2. Neural gene expression analysis, confirmed effects on 18 out of 30 genes previously found to affected after exposure to higher doses to the same pollutants. Our findings indicate that exposure to POP at low doses is associated with subtle, but toxicological relevant effects on post-natal development in female mice.

Abbreviations

ACTB	actin, beta
AhR	aryl hydrocarbon receptor
AHR	activation of the Aryl Hydrocarbon Receptor
Arnt	aryl-hydrocarbon receptor nuclear translocator 2
Arntl	aryl hydrocarbon receptor nuclear translocator-like
ARPC2	actin-related protein 2/3 complex subunit 2
ATP5B	ATP synthase, H+ transporting, mitochondrial F1 complex, beta polypeptide
BBB	blood brain barrier
BFR	brominated flame retardants
BFR	brominated flame retardants
BVA	Biological Variation Analysis
Ca2+	calcium
CAR	constitutively active/androstane receptor
CB-153	2,4,5,2',4',5'-hexachlorobiphenyl
CYP	cytochrome P450
DIA	Differential In-Gel Analysis
DIGE	difference in gel electrophoresis
DL	dioxin like
Dnajb5	DnaJ Hsp40) homolog, subfamily B, member 5
DNM1	dynamin 1
DPYSL3	dihydropyrimidinase-related protein 3
E2	17ß-oestradiol
Eapp	E2F-associated phosphoprotein
EFSA	European Food Safety Authority
Eif5	eukaryotic translation initiation factor 5

ACCEPTED MANUSCRIPT

emPAI	exponentially modified protein abundance indice
ENO1	alpha-enolase
EU	European Union’s
G6PD	and glucose-6-phosphate dehydrogenase
GAPDH	glyceraldehyde-3-phosphate dehydrogenase
HBCD	1,2,5,6,9,10-Hexabromocyclododecane
HD	high dose
HSPA8	heat shock 70kDa protein 8
Hspa8	heat shock 70kDa protein 8
IEF	Isoelectric focusing
IPA	Ingenuity Pathway Analysis
IVD	isovaleryl-CoA dehydrogenase, mitochondrial
JECFA	Joint FAO/WHO Expert Committee on Food Additives
LC-MS/MS	Liquid chromatography tandem mass spectrometry
LD	low dose
LOAEL	lowest observed adverse effect levels
Lztfl1	leucine zipper transcription factor-like 1
MAPK14	mitogen-activated protein kinase 14
MOE	margin of exposure
Mterfd2	mitochondrial transcription termination factor 4
Mtf1	metal-regulatory transcription factor 1
NDL	non-dioxin like
NfkB	nuclear factor kappa B
NOAEL	no observed adverse effect level
Nr1i3	nuclear receptor subfamily 1, group I, member 3
Nsdhl	NAD P) dependent steroid dehydrogenase-like
PCBs	polychlorinated biphenyls
Pnkd	paroxysmal nonkinesigenic dyskinesia
POP	persistent organic pollutants
PXR	pregnane X receptor
qPCR	quantitative polymerase chain reactions
RALA	v-ral simian leukemia viral oncogene homolog A ras related
SCF	European Commission's former Scientific Committee for Food
SIRT2	NAD-dependent deacetylase sirtuin-2
Slc30a3	solute carrier family 30 zinc transporter), member 3
Sphk2	sphingosine kinase 2
Srrm2	serine/arginine repetitive matrix 2

ACCEPTED MANUSCRIPT

ACCEPTED MANUSCRIPT

T	Testosterone
T/E2 - ratio	Testosterone/17ß-oestradiol ratio
Tarsl2	threonyl-tRNA synthetase-like 2
TCDD	2,3,7,8-tetrachlordibenzo-p-dioxin
TEQWHO	toxic equivalency quotient
Tnfsf12	tumor necrosis factor ligand) superfamily, member 12
TUB2A	tubulin beta-2A chain
TWI	tolerable weekly intake
US EPA	United States Environmental Protection Agency
Zn2+	zinc

Keywords: POP; endocrine disruption; neurotoxicity; calcium; zinc; G6PD; oestradiol; liver

1. Introduction

Persistent organic pollutants (POP) are bioaccumulating and biomagnifying environmental contaminants that resist degradation in the environment and are a major concern to human health [1].

The Brominated flame retardant (BFR) 1,2,5,6,9,10-Hexabromocyclododecane (HBCD) has become a ubiquitous environmental contaminant and is detected at increasing levels in human adipose tissue, serum, breast milk and human fetal tissue [2]. Due to its adverse effects on human health and the environment, HBCD has been listed under the Stockholm convention on POP in Annex A (POP for elimination) with the specific exceptions that HBCD can be still produced and used for expanded polystyrene and extruded polystyrene in buildings [3]; thus, environmental exposure to HBCD is likely to persist. Among population subgroups within the EU, children (3-10 years old) have been reported to have the highest intake of HBCD [4]. Knowledge of the toxicodynamics of HBCD has increased in recent years, but is still limited [5]. HBCD can cause histological damage to liver, thymus and thyroid, and adversely affect thyroid hormone levels and thyroid hormone receptor-mediated gene expression [4,6–8]. In a combined *in vivo* and *in vitro* transcriptomics study in mice, the hypothalamus-hypophysis-gonadal axis was a major target of HBCD exposure [3]. Accordingly, reproductive toxicity of HBCD has been reported in both male and female rats [4,9]. HBCD has effects on memory and learning [6,10], which may be caused by impaired dopamine and glutamate re-uptake, and disruption of calcium (Ca^{2+}) and zinc (Zn^{2+}) signalling in glutamatergic neurons [3,11,12]. Neurodevelopmental effects on behaviour in mice was selected as the critical effect by the European Food Safety Authority (EFSA) in their risk assessment on HBCD [4].

The polychlorinated biphenyl (PCB) 2,4,5,2',4',5'-hexachlorobiphenyl (CB-153) was shown to induce adverse effects in a number of target tissues including the thyroids, reproductive system, liver and brain [13]. CB-153 may affect biological systems through mechanisms including disruption of cellular Ca^{2+} homeostasis [14], and activation of both the constitutively active/androstane receptor (CAR) and the pregnane X receptor (PXR) [15]. For CB-153, EFSA established a no observed adverse effect level (NOAEL) of 1.2 mg kg^{-1} bw d^{-1}, based on hepatotoxicity in rats as the critical effect [13]. More recently, based on 28

ACCEPTED MANUSCRIPT

and 90 days repeated dose exposure studies, the Joint FAO/WHO Expert Committee on Food Additives (JECFA) estimated the NOAEL for effects on liver and thyroid for CB-153 to be 10 µg kg^{-1} bw d^{-1} and calculated an estimated margin of exposure (MOE) of 1600 - 3100 for adults [16]. Other health based guidance values such as a tolerable weekly intake (TWI) for CB-153 are, due to a general lack of *in vivo* toxicity data, yet to be established [13,16].

Dioxins including as 2,3,7,8-tetrachlordibenzo-p-dioxin (TCDD) and dioxin-like (DL) PCBs are thoroughly investigated POP with targets of toxicity including the reproductive and the immune system [17] as well as the brain, affecting neurodevelopment, cognitive faculties and motor function [18–20]. Dioxins exert toxicity through binding to and activation of the Aryl Hydrocarbon Receptor (AHR) [21], which controls a large battery of genes including members of the cytochrome P450 (CYP) family [22], the nuclear factor kappa B (NfkB) [23] and sex steroid receptors [24,25]. The European Commission's former Scientific Committee for Food (SCF) established a LOAEL for TCDD of 25 ng kg^{-1} bw d^{-1} based on reproductive toxicity after subcutaneous exposure in rats and established a TWI for dioxins and DL PCB of 14 pg kg^{-1} bw d^{-1} [26]. More recently, the United States Environmental Protection Agency (US EPA) set a reference dose which was three-fold lower than the TWI established by the SCF. Currently, EFSA is in the process of re-evaluating and updating the health based guidance value for dioxins and DL PCBs [27].

Exposure to POP during childhood is considered of particular importance as the developing organism for the first time experiences direct exposure to contaminants in the environment and the diet without the mediation of maternal metabolism occurring in pregnancy or lactation [28]. Due to the specific vulnerability and susceptibility of this life stage, children may thus experience greater risks from exposure compared to adults [29]. Using a rodent juvenile model of toxicity our team previously assessed endocrine and histological changes in multiple organs alongside transcriptomic and proteomic responses following dietary exposure to HBCD, CB-153 or TCDD at doses close to their respective lowest observed adverse effect levels (LOAEL) in mice [7,18]. We found adverse effects on livers, thyroid and immune system and altered sex steroid balance [7]. We also found that these POP accumulate in the juvenile brain where TCDD and HBCD caused dysregulation of the otherwise tightly controlled homeostasis of Ca^{2+} and Zn^{2+} [3,18].

While the aforementioned work was done appropriately for the study of dietary early life exposure [30], the concentrations of HBCD, CB-153 and TCDD used in the experimental diets were much higher than the levels usually detected food. In the present work, we assessed systemic responses observed in the same juvenile toxicity model after 28-day repeated dose exposure to dietary relevant concentrations of HBCD, CB-153 and TCDD. Based on the findings from our previous study, which we carried out at approximately 100 (CB-153 and TCDD) to 4000-fold (HBCD) higher doses but otherwise under identical conditions, we paid special attention to endocrine disruption and neurotoxicological effects in developing female juvenile BALB/c mice.

2. Materials and Methods

2.1 Animals

To assess the toxicity of environmentally realistic doses of HBCD, CB-153 and TCDD an animal exposure experiment was conducted at King's College London (KCL) in accordance with the project license guidelines (PPL70/6407) granted under the UK Home Office Animals (Scientific Procedures) Act, 1986. The experimental protocol for juvenile toxicity studies was performed as described in [7,18]. In short, 40 22-day old female BALB/c mice (average weight 13 to 15 g) purchased from Charles River (UK) were housed in Utemp1284 mouse cages (Tecniplast, UK) with wood chips bedding (Aspen-wood chips, B

ACCEPTED MANUSCRIPT

and K Ltd) in rooms controlled for temperature (20 °C to 22 °C), relative humidity (45 % to 65 %), and lighting (12 hour light/dark cycle). After an acclimation period of three days, mice were allocated at random into experimental diet groups. Mice were provided with water ad libitum but feed intake was restricted to 15 % (w/w) kg^{-1} bw day^{-1} to provide for an animal model, which more closely resembles dietary intake of healthy human individuals [31–33]. Throughout the feeding experiment, the general health status of mice was assessed daily and food consumption and body weight gain were recorded weekly and are presented as means ± Standard Deviation (SD). Differences among groups were determined by one-way ANOVA using GraphPad Prism (GraphPad, US). In accordance with Home Office regulation for use of animals in research, we used as few animals as possible to obtain the required results and the number of animals in each group was based on results from previous experiments [7, 18]. Because of loss of tissue for some analyses all analyses did not have the same number of biological replicates and the number of animals used for each analysis has been summarised in Table S1.

2.2 Experimental diets

To closely reflect human exposure to the model POP through marine food sources, which are major contributors to HBCD, CB-153 and TCDD exposure, fish-based experimental diets were prepared as previously described [7,18,34]. In brief, diets were formulated in accordance with the standard rodent diet formulation AIN-93 G and divided into four equal parts of which one part was used as control. The remaining three parts of the diet were spiked with 10 ng g^{-1} CB-153, 335 ng g^{-1} HBCD and 6 pg g^{-1} 2,3,7,8-TCDD, respectively. Prior to the start of the animal experiment, the diets produced were analysed for their contaminant content as described by Maranghi et al. [7].

2.3 Rationale for dose selection

Using the same fish based diets as vehicles, our group previously described the effects of HBCD, CB-153 and TCDD at their respective LOAELs of 199 mg kg^{-1} bw day^{-1}, 195 µg kg^{-1} bw day^{-1} kg-1 bw day^{-1} and 90 ng kg^{-1} bw day^{-1} [7,18]. In the present work, juvenile female BALB/c mice from the same cohort were exposed to diets spiked with 334.64 ± 79.21 ng g^{-1} HBCD, 10.13 ±0.81 ng g^{-1} CB-153 and 6.06 ±0.49 pg g^{-1} TCDD. The selected concentration of HBCD lies within the range of concentrations detected in fish caught in urban Europe, which range from 10 to 1000 ng g^{-1} [35]. The concentration of CB-153 is comparable with levels detected in fatty fish from the Baltic Sea, which were found to contain up to 1.6 ng CB-153 g^{-1} wet weight [13]. The concentration of TCDD in the feed corresponds to the highest mean levels of dioxins detected in eels, 6.7 pg TEQWHO98 g^{-1} wet weight [36].

2.4 Tissue sampling and processing

Tissue sampling and processing were performed as previously described [7,18]. In short, after 28 days of exposure, mice were anaesthetised with Isoflurane (5% mix with oxygen) and placed under an anaesthetic delivery mask. Blood was collected by cardiac puncture; then the anaesthetised animals were sacrificed by cervical dislocation. Brain, liver, spleen, thymus, thyroid and uterus were sampled and weighed. Following dissection and necropsy, left cortices of the brain were flash-frozen in liquid nitrogen, ground in a liquid nitrogen cooled mortar and pestle and processed further as protein and gene extraction methods dictated. Right cortices of the brain and all other tissue samples were fixed in 10% (v/v) buffered formalin and following storage in 80% ethyl alcohol embedded in paraffin prior to histological and histomorphometrical analyses. Differences among groups were assessed by one-way ANOVA using GraphPad Prism (GraphPad, US).

ACCEPTED MANUSCRIPT

2.5 Histological, and histomorphometrical analyses

Histological and histomorphometrical analyses were performed as previously described [7]. In short, paraffin embedded tissues were cut into 5 µm sections and stained the specimens with haematoxylin and eosin for examination under a light microscope (Nikon Microphot FX) with different lenses. Thyroid, adrenals, spleen, thymus and uterus also were subjected to quantitative histomorphometrical analysis. Briefly, slides of selected tissues were examined by using an image analysis system (Nis-Elements D) applied to an optical microscope (Nikon Microphot FX). For the uterus, the ratio between the area of endometrium and myometrium as relative percentage of both uterine tissue components were determined. For thyroids, the follicular density, as ratio between number of follicles and a predetermined thyroid area was determined. In addition, indirect follicular cell height as the mean ratio of follicle and colloid area in five randomly selected follicles/sample was assessed. In the same follicles, the mean ratio of follicular epithelium areas and number of nuclei were calculated as an indicator of follicular maturation. Follicular cell height was estimated as the mean of five cell heights in five randomly selected follicles/sample. For adrenals the ratio between area of cortex and medulla was calculated. For the thymus the ratio between area of cortex and medulla was calculated and for the spleen the ratio between red pulp and white pulp areas was determined.

Histological data are presented as proportions of quantal data (% presence) and analysed by pairwise comparisons of treated groups with control group by means of two-tailed Fisher Exact Test. Histomorphometrical data (mean ± SD) were analysed by the Mann Whitney U-test. We considered differences between groups significant at the $p \leq 0.05$ level.

2.6 Hormone measurements

Steroid hormone analysis was performed as described by Maranghi et al. [7]. In short, serum for the analysis of Testosterone (T) and oestradiol 17β (E2) levels was obtained through centrifugation of coagulated blood samples. Serum levels were measured using radioimmunoassay kits (DPC-coat-a-count Total Testosterone kit and DSL-4400 Oestradiol RIA kit). Hormone data are presented as means ± SD and differences among groups were assessed by one-way ANOVA using GraphPad Prism (GraphPad, US).

2.7 Protein extraction and quantitative intact proteomics analysis

Protein extraction and quantitative intact proteomics analysis were performed as described by Rasinger et al. 2014 [18]. In brief, proteins were extracted using the Sample Grinding Kit with a standard 2 x DIGE Lysis Buffer. Lipids and nucleic acids were removed from the samples using acetone precipitation and protein pellets were re-suspended in DIGE Labeling Buffer. Following protein quantitation (2D Quant Kit) control (n=6), CB-153 (n=6), HBCD (n=6) and TCDD (n=6) treated samples were labelled with 200 pmol fluorescent cyanine dyes using the minimal CyDyeTM DIGE Fluors Cy3 and Cy5 in a symmetrical dye-swap design. In addition, we mixed excess control (n=6) and treated (n=24) samples in a 1:1 ratio to produce internal standard (IS). IS was Cy2TM (CyDyeTM DIGE Fluor) labelled for DIGE and used in bulk on preparative gels, respectively. Randomly selected Cy3 and Cy5 labeled samples were combined with Cy2TM labeled IS and cup-loaded onto IPG strips. Isoelectric focusing (IEF) was performed on an IPG Phor II run at 75 µA/IPG strip for 60 kVh at 20 ºC. Upon completion of the IEF, equilibrated IPG strips were subjected to polyacrylamide gel electrophoresis using using polyacrylamide gels cast in house. Following the electrophoretic separation of the CyDyeTM – labeled proteins, we imaged the gels

ACCEPTED MANUSCRIPT

immediately using an Ettan DIGE Imager. Aquired images were subjected to data analyses using the DeCyderTM 2D, the BioConductor package Limma and the Qlucore Omics Explorer. Only protein spots were considered for mass spectrometry (MS) identification that were identified as differentially expressed at the $p<0.01$ level in at least two of the three statistical analyses performed. In addition, we also identified a subset of proteins significant at $p<0.05$ to facilitate pathway analysis and to allow for validation of Ingenuity Pathway Analysis (IPA) predicted changes in the expression data set.

2.8 Protein mass spectrometry and proteomics bioinformatics analysis

Protein MS and proteomics bioinformatics analysis was performed as described by Rasinger et al. [18]. In brief, gel spots containing the differentially expressed proteins were excised from preparative 2D gels and digested with sequencing grade trypsin using an Investigator ProGest robotic digestion system [37,38]. Tryptic peptides were separated by reverse phase nano-flow liquid chromatography and subjected to online tandem mass spectrometry analysis via a nano-spray source. Spectra were collected from the mass analyser using full ion scan mode over the m/z range 450 - 1600. Six dependent tandem MS (MS/MS) scans were performed on each ion using dynamic exclusion. The obtained MS/MS data were matched to database entries using the SEQUEST algorithm in Bioworks and then exported the data to Scaffold. Carboxyamidomethylation of cysteine was used as a fixed modification, and oxidation of methionine was used as a variable modification. The mass tolerance was set at 10 ppm for the precursor ions and at 1 AMU for fragment ions. Two missed cleavage sites were allowed. We loaded search results into Scaffold software where protein and peptide probabilities were computed. Assignments were accepted with > 99.0% protein probability, > 95.0% peptide probability, and a minimum of two peptides [39,40]. If we detected co-migration of proteins in one single spot exponentially modified protein abundance indices (emPAI) [41] as implemented in Mascot were calculated to determine the relative abundance of each protein present in the spot. The search settings we used in the Mascot were identical to ones used in Bioworks described above. Biological network analysis was performed to concomitantly interpret the proteomics data. Uniprot-Swissprot Accession numbers of identified differentially expressed ($p<0.05$) proteins were uploaded into the Ingenuity Pathway Analysis software suite (IPA, Ingenuity Systems, USA). Successfully mapped proteins were subjected to an IPA Core Analysis using default settings followed by targeted upstream regulator analysis.

2.9 RNA extraction and qPCR analysis

Total RNA was extracted from the brain using Trizol (Invitrogen, Life Technologies, USA) and the Qiagen RNeasy-Mini kit (Qiagen, Canada). RNA purity was assessed using a Nanodrop ND-100 UV-Vis Spectrophotometer (Nanodrop Technologies, USA) and RNA quality and integrity using the Agilent 2100 Bioanalyzer in combination with the RNA 6000 LabChip kit (Agilent Technologies, USA). Expression levels of mRNA were measured by quantitative polymerase chain reactions (qPCR) on an ABI Prism7900 instrument, using either SYBR green or hydrolysis probe assays. cDNA was synthesised from 5 µg of total RNA using random primers and SuperScript™ III (Invitrogen). Following cDNA synthesis and RNA degradation by RNase H, cDNA was stored at -20°C until used. The GeNorm mouse housekeeper selection kit was used (Primerdesign) and cytoplasmic beta actin (ACTB) identified as the least variable transcript among six candidates in 15 randomly selected samples covering exposure to each of the four POP. qPCR experiments were run for 31 gene targets deploying pre-validated assays (Roch Diagnostics) based on Universal ProbeLibrary (UPL) short hydrolysis probes, substituted with locked nucleic acids. Samples from five animals per condition were analysed in quadruplicate technical replicates for each

ACCEPTED MANUSCRIPT

of the 31 transcripts and for the housekeeping gene ACTB. Expression of transcripts analysed using UPL was statistically assessed using pairwise comparisons of dCt (cycle threshold target – cycle threshold HKG) values against the control group with the Qlucore Omics Explorer software (Qlucore, Sweden). In all cases, the data were expressed as fold-change (FC) relative to the control group with statistical significance (ANOVA) accepted at $p<0.01$ and $p<0.05$.

3. Results

3.1 Chemical analysis, general observations and necropsy findings

Juvenile female BALB/c mice fed the: (i) HBCD spiked diet (334.64 ± 79.21 ng HBCD g^{-1}) were exposed to 49.5 μg HBCD kg^{-1} bw-1 day^{-1}; (ii) mice fed the CB-153 spiked diet (10.13 ±0.81 ng g^{-1}) to 1.35 μg CB-153 kg^{-1} bw^{-1}, and (iii) mice fed the TCDD spiked diet (6.06 ±0.49 pg g^{-1}) to 0.90 pg TCDD kg^{-1} bw^{-1}. During exposure, we recorded no differences in feed consumption or weight gain. No effects were observed at the time of sampling concerning final body weight, target organ weights, somatic indices of the liver, spleen or thymus; no gross lesions or other treatment-related changes were observed at necropsy.

3.2 Histopathological findings and hormone measurements

In mice exposed to HBCD the livers showed significantly ($p<0.05$) increased vacuolation in hepatocytes (62%), lymphocytic infiltration (+75%), and hyperaemic vessels (+75%); in addition, the thymus showed significantly ($p<0.05$) increased signs of tissue stress (+50%) and the uterus a significant increase of the incidence of reduced density of endometrial glands (Table 1). Follicles with larger cells were present in the thyroid, as shown by a significantly increased ($p <0.05$) ratio between follicular epithelium areas and number of nuclei (+20%) (Table 2). No significant effects on histology were observed in adrenals, brain and spleen. In the HBCD-exposed group the serum concentration of oestradiol 17β was significantly ($p<0.05$) lower and the testosterone to oestradiol 17β ratio (T/E2 - ratio) was significantly ($p<0.05$) higher than the control group (Figure 1).

In the animals exposed to CB-153, we observed a significant increase in lymphocytic infiltration (+50%, $p<0.05$) in the livers and a significant ($p<0.05$) increase in tissue stress (+70%) in the thymus (Table 1). Thyroid follicles had larger cells, as shown by the significantly ($p<0.05$) increased ratio of follicular epithelium areas and number of nuclei (+36%) (Table 2). Testosterone levels were significantly increased in this group (Figure 1).

In the animals exposed to TCDD we detected a significant ($p<0.05$) increase in lymphocytic infiltration (+50%, $p<0.05$) in the livers (Table 1); no significant changes were observed in the measured hormone levels; however, similar to HBCD and CB-153, a numeric increase of the T/E2 - ratio was observed (Figure 1).

3.3 Differential protein and gene expression analysis

We detected significant ($p<0.01$) quantitative differences in protein expression in the brains of the POP-exposed groups in comparison with controls, namely: (i) four proteins differentially expressed in brains of HBCD-exposed mice, (ii) four proteins in the CB-153 exposed group, and (iii) 12 proteins in mice exposed to TCDD (Figure 2). Proteins reproduced successfully on preparative 2D gels were identified by LC-MS/MS (Figure 3). In addition to proteins displaying significant differences in expression level at the $p<0.01$

ACCEPTED MANUSCRIPT

level we also identified a subset of proteins significant at $p<0.05$ to facilitate pathway analysis and to allow for validation of IPA predicted changes in the expression data set. To differentiate between the two sets, proteins significant at the $p<0.01$ level are marked with an asterisk (*). Relevant protein expression data including protein spot identifiers, statistical significance, fold changes, and protein identification features including accession number, isoelectric points, molecular weights, Mascot protein score and emPAI are presented in Table S2A and S2B.

Further analysis of identified differentially expressed proteins revealed both unique and overlapping responses to the three pollutants (see Figure 4). Exposure to HBCD triggered unique abundance changes in heat shock 70kDa protein 8 (HSPA8; -1.29*), isovaleryl-CoA dehydrogenase, mitochondrial (IVD; -1.16*), mitogen-activated protein kinase 14 (MAPK14; -1.26) and v-ral simian leukemia viral oncogene homolog A (ras related) (RALA; 1.17*). Exposure to CB-153 elicited unique significant changes in dynamin 1 (DNM1; 1.39). Exposure to TCDD triggered unique significant changes in dihydropyrimidinase-related protein 3 (DPYSL3; 1.11), ATP synthase, H^+ transporting, mitochondrial F1 complex, beta polypeptide (ATP5B; 1.16), alpha-enolase (ENO1; 1.15), actin, beta (ACTB; -1.21*) and glyceraldehyde-3-phosphate dehydrogenase (GAPDH; 1.28) Two proteins were observed to share significant changes in abundance after exposure to HBCD and TCDD, respectively namely, NAD-dependent deacetylase sirtuin-2 (SIRT2; 1.13 and 1.27*) and actin-related protein 2/3 complex subunit 2 (ARPC2; 1.18 and 1.18). Two proteins namely, tubulin beta-2A chain (TUB2A; spot 415: -1.3 and -1.3 and spot 458: -1.14*) and glucose-6-phosphate dehydrogenase (G6PD; -1.29*,-1.26*,-1.25*) had significantly altered expression levels after exposure to all three POP.

In addition to exploratory proteomics analysis, we screened a total of 30 genes for differential expression levels in brain of mice exposed to the test compounds compared with the control (see Figure 5). The target genes, were chosen based on our previous data representing cellular pathways found to be affected by one or several of the three pollutants at higher doses [18] and from association with at least one of the toxicants in the Comparative Toxicogenomics Database (CTD) [42]. In accordance with the proteomics data, we screened for significantly differentially expressed genes at both the $p<0.01$ and $p<0.05$ level. To differentiate between the two sets, genes significant at the $p<0.01$ level are marked with an asterisk (*). Of the 30 genes tested, 4* and 7 (HBCD), 2* and 9 (CB-153) and 8* and 4 (TCDD) displayed significant ($p<0.01$* and $p<0.05$) responses in gene expression. Gene expression data including p values, fold change, Entrez Gene Name, cellular location, function for all genes tested are presented in Table S3A. In addition, in Table S3A also the PubMed IDs of publications (as listed in the CTD) which reported differential regulation of the tested genes after exposure to HBCD, CB-153 and TCDD are provided.

In accordance with the protein expression data, both unique and overlapping responses among treatments in all three-exposure conditions were detected in gene expression data (see Figure 4B). Substance-specific responses in gene expression concerned one gene for HBCD, (threonyl-tRNA synthetase-like 2, Tarsl2; -0.44*). Three genes were found to be dysregulated after exposure to CB-153, namely solute carrier family 30 (zinc transporter), member 3 (Slc30a3; -0.23), mitochondrial transcription termination factor 4 (Mterfd2; -1.23) tumor necrosis factor (ligand) superfamily, member 12 (Tnfsf12;) and two genes for TCDD, namely nuclear receptor subfamily 1, group I, member 3 (Nr1i3; 1.42*), DnaJ (Hsp40) homolog, subfamily B, member 5 (Dnajb5; 1.23). Differential expression of leucine zipper transcription factor-like 1 (Lztfl1) and aryl-hydrocarbon receptor nuclear translocator 2

ACCEPTED MANUSCRIPT

(Arnt) was observed after exposure to either HBCD (Lztfl1: -0.64*; Arnt: -1.54) or CB-153 (Lztfl1: -0.50; Arnt: -1.43). Differential expression of metal-regulatory transcription factor 1 (Mtf1), NAD(P) dependent steroid dehydrogenase-like (Nsdhl), serine/arginine repetitive matrix 2 (Srrm2) and heat shock 70kDa protein 8 (Hspa8) was detected after exposure to either HBCD (Mtf1: 3.27; Nsdhl: 2.96; Srrm2: 2.90; Hspa8: 2.8) or TCDD (Mtf1: 1.97*; Nsdhl: 1.75*; Srrm2: 1.71*; Hspa8: 1.31). Differential expression of paroxysmal nonkinesigenic dyskinesia (Pnkd) and aryl hydrocarbon receptor nuclear translocator-like (Arntl) after exposure to either CB-153 (Pnkd: 0.88; Arntl: 0.643) or TCDD (Pnkd: 0.96*; Arntl: 0.71). The genes E2F-associated phosphoprotein (Eapp), eukaryotic translation initiation factor 5 (Eif5), sphingosine kinase 2 (Sphk2) and aryl hydrocarbon receptor (AhR) were found to be differential expressed after exposure to HBCD (Eapp: -1.25*; Eif5: -3.22*; Sphk2: 2.95; AhR: 2.75), CB-153 (Eapp: -1.09*; Eif5: -3.03*; Sphk2: 2.09; AhR: 1.97) or TCDD (Eapp: -1.07*; Eif5: -1.92*; Sphk2: 1.74 ; AhR: 1.67*).

2.3 Proteomics functional analysis and bioinformatics

The Ingenuity Pathway Analysis (IPA) platform was used with default settings to group proteins into larger functional categories (Table S4A–D). Similar to the differences observed in individual protein and gene expression induced by the three different POP, distinct and overlapping responses were detected at the pathway level (Figure 5). The functional categories "clathrin mediated endocytosis signalling" and "remodelling of epithelial adherens junctions" were significantly ($p<0.05$) affected by all three POP under investigation; "sertoli cell-sertoli cell junction signalling" and "sirtuin signalling" after exposure to HBCD and TCDD.

To elucidate the early events upstream, the predicted effects on cellular and tissue biology of the juvenile brain, an "upstream regulator analysis" was performed in IPA. This analysis revealed that changes observed in the brain of mice exposed to HBCD and TCDD are linked to decreased 'beta-estradiol' (Figure 6A and 6B, respectively). No prediction could be made for CB-153.

4. Discussion

Risk assessment agencies call for data on the effects of direct exposure of children and infants to environmental contaminants including POP [28]. The diet, and oily fish in particular, represent a major route of exposure to HBCD, CB-153 and TCDD [43,44]. In the present study, using a fish based diet as vehicle, we describe systemic responses observed in juvenile female BALB/c mice after 28 days short-term repeated low-dose (LD) exposure to HBCD (49.5 μg kg^{-1} bw^{-1} day^{-1}), CB-153 (1.35 μg kg^{-1} bw^{-1}) or TCDD (0.90 pg kg^{-1} bw day^{-1}). In accordance with high-dose (HD) data we published earlier from this experiment in which mice were exposed to 199 mg HBCD kg^{-1} bw day^{-1}), 195 μg CB-153 kg^{-1} bw day^{-1} and 90 ng TCDD kg^{-1} bw day^{-1}) [7,18], we put special attention on endocrine disruption, histopathologic and neurotoxicological effects in developing juvenile female BALB/c mice; a model appropriate for the study of early life dietary exposure [30].

4.1 Histopathological findings and hormone measurements

Histology data indicated that the thyroid displayed subtle alterations upon exposure to HBCD and CB-153 at both LD (present study) and HD [7] and upon exposure to TCCD at

ACCEPTED MANUSCRIPT

HD exposure only [7]. The larger cells observed in thyroids of mice exposed to HBCD LD and CB-153 LD (present study) show that the thyroid is affected by HBCD and CB-153 at doses below the LOAELs previously established for juvenile mice [7]. As expected, structural changes were more evident at HD levels; and CB-153, a recognized inducer of thyroid toxicity [45], elicited effects at much lower exposure levels (both HD and LD) than HBCD. While POP-induced follicular cell hypertrophy can be reversed by a long-term withdrawal of POP exposure [46], early-onset and prolonged thyroid dysfunction can severely impact female reproductive health [47]. Both LD (present study) and HD exposure [7] to HBCD increased the incidence of marked vacuolation in hepatocytes; no such effect was observed after LD exposure to CB-153 or TCDD. This finding supports the hypothesis that lipid metabolism in liver is affected by HBCD in juvenile female mice [2]. The histology data indicated further that lymphocyte infiltration was increased in livers of mice after exposure to LD levels (present study) of HBCD, CB-153 or TCDD. At HD exposure livers of mice exposed to HBCD and CB-153 also displayed lymphocyte infiltration [7], whereas this change was absent in TCDD-treated mice. Lymphocyte infiltration suggests an ongoing persistent inflammation of the liver such as that observed in autoimmune hepatitis [48]. The increased occurrence of pyknotic nuclei, a hallmark of apoptosis [49], was not observed at LD (present study) whereas at HD was present only in livers of TCDD exposed mice [7]. These findings suggest that TCDD may induce different adverse effects in juvenile livers at different dose levels; direct hepatocyte toxicity, as evidenced by the increase of isolated necrotic hepatocytes (pyknotic nuclei) at HD, and chronic inflammation at LD exposure. The livers of HBCD LD exposed mice in the present study presented a noticeable association between hepatocyte vacuolation and chronic liver inflammation both features of non-alcoholic fatty liver disease, a manifestation of the metabolic syndrome which is increasingly associated with exposures to environmental chemicals [50]. Our data thus highlights the need for further investigations on the hepatotoxic effects of POP such as HBCD at real-life exposure levels; the possible dose-dependency of TCDD-induced liver toxicity also deserves attention.

The data we obtained on thymus indicates that the immune system of juvenile female mice may be a target of POP toxicity. Indeed, increased signs of tissue stress were observed in the thymus of mice exposed to all three contaminants tested at both LD (present study) and HD [7]. Interestingly, accelerated thymus regression can be related to sexual steroid stimulus [51]. In spleen histological changes were observed only at HD after exposure to CB-153 [7]. This indicates that spleen tissue may be less susceptible to POP exposure than thymus.

Uterine histo-architecture showed a significantly decreased endometrial gland density upon exposure to LD HBCD (present study). Changes in circulating oestradiol 17β can modulate endometrial gland differentiation in mammals [52]. In fact, LD HBCD exposed mice showed a significant decrease in oestradiol 17β and a numerical decrease of testosterone concentration. In the previous HD study, HBCD induced only a numerical reduction of oestradiol while serum testosterone was significantly increased [7]. Ultimately, the T/E2 ratio was significantly increased at both LD (present study) and HD HBCD exposure [7].

Data on the endocrine mode of action of HBCD are scarce. In *in vitro* experiments HBCD displayed both anti-androgenic and anti-oestrogenic activity in CALUX® sex steroid receptor reporter gene assays and anti-oestrogenic activity in a MCF-7 cell proliferation assay [53,54]. Our data suggest that *in vivo* HBCD may elicit toxicologically relevant alterations of sex steroid balance at a dose below the LOAEL previously established for juvenile mice [7]. The T/E2 ratio upon TCDD exposure showed an apparent dose-related pattern, with a significant increase at HD [7] and a numerical, non-significant increase at LD (present study). Exposure to LD CB-153 significantly increased the serum testosterone levels and numerically increased the T/E2 ratio; at HD CB-153 exposure no difference from the control

ACCEPTED MANUSCRIPT

groups was detected [7]; the possible relevance of this finding, e.g., with regard to a non-monotonic dose-response relationship [55] warrant further investigation.

4.2 Effects on murine brain gene and protein expression levels

We assessed if exposure to the three contaminants HBCD, CB-153 and TCDD at LD induces differences in gene expression. Based on our previous work and genes of interest focusing on regulation of Ca^{2+} and Zn^{2+} selected from the CTD, a set of 30 target genes were analysed by qPCR. Of these 30 genes, eight (Ahr, Eapp, Eif5, Mtf1, Nr1i3, Nsdhl, Pnkd and Srm2), two (Eapp and Eif5) and four (Eapp, Eif5, Lztfl1 and Tarsl2) genes also were significantly differentially expressed after LD exposure to HBCD, CB-153 and TCDD, respectively. This confirmed that effects previously found to be affected at HD exposure were in parts reproducible in brains of mice exposed to doses below the LOAEL previously established in juvenile mice [7]. Moreover, these data highlight that already at LD exposure levels POP may interfere with the tightly controlled homeostasis of Ca^{2+} and Zn^{2+} in the juvenile brain.

In addition to gene expression analysis, we performed a gel-based exploratory proteomics on brain tissue of POP exposed mice. Omics analyses allow for experiments which can implicate molecular networks affected by chemicals and help elucidating molecular initiating and key events in adverse outcome pathways [56]. Omics profiling is performed without prior hypothesis and is often considered as unbiased and discovery driven [3,57]. DIGE based proteomics analysis after exposure to HBCD, CB-153 and TCDD at the LD level (present study) induced dysregulation of three (HSPA8, G6PD and SIRT2), one (G6PD) and four (G6PD, TUB2A, ACTB and RALA) proteins, respectively. The protein, G6PD, was downregulated after LD exposure to all of the three POP. This is noteworthy because G6PD is a regulatory enzyme in the NADPH-dependent biotransformation of xenobiotics [58]. Its expression levels and activity determine the NADPH levels whose reductive power protects cells against reactive oxygen species (ROS)-induced oxidative stress damage [59]. Recently, a mechanistic link between increased G6PD activity, elevated NADPH and redox potential and improved antioxidant protection was established in transgenic mice with a modest overexpression of G6PD [59]. Conversely, a chemically induced G6PD reduction may thus increase the susceptibility to oxidative damage in the brain as was observed in G6PD deficient mice which displayed high levels of oxidative damage in the brain [60].

The downregulation of G6PD protein, in the TCDD LD exposed mice, was accompanied by an upregulation of SIRT2 protein. This enzyme plays a key role in the dynamic regulation of G6PD helping cells to sense oxidative stress and to maintain NADPH homeostasis through G6PD acetylation in a SIRT2 dependent manner [61]. This finding provides further evidence that in cells in the brain are under at a least mild oxidative stress TCDD-exposed juvenile female BALB/c mice, since SIRT2 is not up-regulated in unstressed cells [61]. Oxidative damage in the brain plays a key role in the functional decline of this organ system and predisposes it to vascular- and degenerative damage [62,63]. As early life exposure to POP affects learning and memory functions in adult mice [64], the dysregulation of oxidative stress sensors in the brains of a juvenile mouse model warrants further research.

Besides oxidative stress related pathologies, G6PD deficiency was also highlighted to be a primary cause of decreased cholesterol anabolism and fatty acid β-oxidation; both of which are key to processes and functions such as plasma membrane formation, energy metabolism and cell signalling [65]. Fatty acid β-oxidation was recently demonstrated to be a target of HBCD toxicity; it was found to be downregulated *in vitro* in HepG2 cells and *in vivo* in livers of juvenile female BALB/c mice after exposure to t-HBCD and α-HBCD, respectively [2,66]. The observed effects on β-oxidation were hypothesised to occur via the suppression of PPAR-α through PXR-related pathways and/or the disruption of the otherwise tightly

ACCEPTED MANUSCRIPT

controlled Ca^{2+} homeostasis [2]. G6PD mediated effects on β-oxidation could provide an additional explanation how POP exposure affects whole body lipid metabolism.

In addition to enzymatic control via SIRT2, the expression levels and activity of G6PD were reported to be under hormonal control and increased in the presence of oestradiol [67,68]. A downregulation of G6PD, for example due to a POP induced altered T/E2 ratio may lead to a distinctly lower NADPH supply in the juvenile brain and consequently weaken its defences against oxidative stress and reduce fatty acid β-oxidation. The data obtained in the present study indicates that the observed downregulation of G6PD after LD exposure to HBCD, CB-153 and TCDD could, at least in part, be related to the significantly (HBCD and CB-153) and numerically (TCDD) increased T/E2 ratios. In addition, since the POP investigated in the present work were shown to pass the blood brain barrier (BBB) and to accumulate in the brain [18], further research could investigate if these xenobiotics might also interfere with the transformation between oestrogens and androgens directly in the brain.

In vertebrates, T/E2 ratios are of great physiological importance and strongly affect the function of both reproductive and non-reproductive organs through various life stages [69]. Increased T/E2 ratios have been associated with metabolic changes such as hyperinsulinemia, impaired liver lipid metabolism and increased risk of cerebrovascular disease [70,71]. T/E2 ratios are determined by the activity of the cytochrome P450 aromatase, a terminal enzyme expressed in various tissues of the body, which irreversibly transforms androgens into oestrogens [72,73]. In the brain, aromatase may play a pivotal role as it was shown that oestrogen is required for the maintenance, survival and the integrity of dopaminergic neurons [74,75]. Aromatization was also recently highlighted to be key for memory and learning in female organisms, which is mediated through both genomic and non-genomic actions of oestrogen [76]. Xenobiotics, which affect the conversion of oestrogen to testosterone and alter the T/E2 ratio, can therefore have a significant impact on brain health and disease [77].

Aromatase was hypothesised to play an important role in the endocrine disruptive potential observed for HBCD, CB-153 and TCDD [10,78,79]. An *in vitro* study pointed out that already at femtomole exposure to TCDD significantly decreased E2 secretion and mRNA expression levels of aromatase were detected in human luteinizing granulosa cells [79]. Interestingly, similar to PPAR-α, which regulates β-oxidation, aromatase activity is also regulated by Ca^{2+}, which strongly inhibits aromatase at high but still physiological concentrations [76]. HBCD, CB-153 and TCDD have previously been reported to disrupt Ca^{2+} homeostasis [12,18,80,81]. In a recent study our team further corroborated Ca^{2+} signalling a sensitive target of HBCD toxicity; in a parallel in vitro and in vivo transcriptomics study in juvenile mice and neuronal N2A and NSC19 cells. [3]. Bioinformatics analysis in the aforementioned study also implicated gene networks in the hypothalamus-hypophysis-gonadal axis and highlighted oestradiol 17β to be significantly regulated in mouse brain and both cells lines at both doses tested.

Changes in Ca^{2+} homeostasis are also involved in the ageing of the brain and contribute to impaired cognition and increased vulnerability to excitotoxicity and neurodegenerative diseases; oestradiol may prevent those and offers neuroprotection even at advanced age [82]. In the present study, in addition to the observed altered serum T/E2 ratios, we observed significant differential down-regulation of HSPA8 and up-regulation of RALA after HBCD exposure and down-regulation of ACTB after TCCD exposure. In line with IPA knowledge base reports, which predict potentially affected upstream regulators from an expression data set, the downregulation of HSPA8 and ACTB and the upregulation of RALA were associated with decreases in oestradiol levels. When applying a less stringent significance cut-off for differential protein expression ($p<0.05$ instead of $p<0.01$), IPA analysis also allowed for the calculation of an activation z-score for oestradiol levels in the brain, which were predicted to be decreased after both HBCD LD and TCDD LD exposure.

ACCEPTED MANUSCRIPT

Taken together, our findings indicate that the POP investigated may disrupt the T/E2 balance in juvenile female mice through disruption of Ca^{2+} homeostasis. This leads to reduced G6PD expression and an associate reduced NADPH supply for xenobiotic detoxification and other cellular antioxidative defence mechanisms in the juvenile brain and increases its susceptibility to oxidative stress injury. In addition, reduced G6PD expression following POP exposure may also result in decreased cholesterol anabolism and impaired β-oxidation in juvenile female BALB/c mice.

4.3 Dose levels, environmental and human relevance

In earlier work our team provided mechanistic data, which indicated known and novel targets of POP toxicity in postnatal development at doses close to published LOAELs in mice [3,7,18]. Having identified these targets in our study system, we wished to investigate if they are also affected at doses more relevant for human exposure during child- and early adulthood.

Of the three chemicals investigated in the present study, the largest margin to human exposure levels was for HBCD. Dietary exposure to HBCD in European countries rarely exceeds 3 ng kg^{-1} bw d^{-1} [4], which is three orders of magnitude below the doses given to mice in the present study. Average daily dietary intakes in Europe of the sum of NDL PCB (PCB6) were reported to be in the range of 10–45 ng kg^{-1} bw d^{-1} for adults with limited exposure data for young children indicating that the average daily intake (breastfeeding excluded) of PCB6 is about 27–50 ng kg^{-1} bw [83]. Thus, the estimated average human exposure to CB-153 is approximately two orders of a magnitude lower than the one used in the present study (1.35 µg CB-153 kg^{-1} bw^{-1}). However, high consumers of fatty fish may have intakes one order of magnitude higher than the median values of the population, as was established for a different POP group [84]. Thus, the exposure level of CB-153 in the present study may be considered to be in line with real-life intake of the 95th percentile consumers. The daily dose of TCDD mice were exposed to in the present study (0.90 pg kg^{-1} bw^{-1}) is similar to the average sum of dioxins and DL PCB exposure between 1.08 and 2.54 pg WHO_{05}-TEQ kg^{-1} bw estimated in European toddlers and other children [85].

Conclusions

In the present study, for the first time it has been shown that exposure to HBCD, CB-153, or TCDD through a fish-based diet is associated with subtle, but toxicological relevant aberrations in histology, endocrinology, protein expression, and gene regulation at doses below the LOAEL previously established in juvenile female mice [7,18]. While the observed effects were not severe their occurrence before the start of sexual maturity should not be overlooked as disruptions during critical phases of development and maturation may in the long term alter the ability of the organism to cope with external stimuli, pregnancy or aging.

Author Contributions: JDR and TSC designed and executed the animal exposure experiment. FM, RT and GM performed the histological analyses and IA and RT conducted the serum biomarker analyses. CH, AKL, and AM were principal investigators and supervised the project. JDR and CH drafted the manuscript and all authors contributed to discussion of the results and writing of the manuscript. Professor Manuel Mayr, Dr. Xiaoke Yin, Dr. Mathew Arno and Dr. Estibaliz Aldecoa-Otalora Astarloa are acknowledged for their excellent technical assistance.

ACCEPTED MANUSCRIPT

Conflicts of Interest: The authors declare no conflict of interest.

Acknowledgments: The study was supported by Aquamax (EU-contract no. 016249-2), a Project funded by the European Commission within the Sixth Framework Programme (www.aquamaxip.eu) and the Project "Seafood and mental health: Uptake and effects of marine nutrients and contaminants alone or in combination on neurological function" (Grant No. 186908/I30) a Project funded by the Research Council of Norway.

ACCEPTED MANUSCRIPT

ACCEPTED MANUSCRIPT

References

[1] P.R.S. Kodavanti, Neurotoxicity of persistent organic pollutants: possible mode(s) of action and further considerations, Dose Response 3 (2006) 273–305.

[2] A. Bernhard, M.H.G. Berntssen, A.-K. Lundebye, A. Røyneberg Alvheim, L. Secher Myrmel, E. Fjære, B.E. Torstensen, K. Kristiansen, L. Madsen, T. Brattelid, J.D. Rasinger, Marine fatty acids aggravate hepatotoxicity of α-HBCD in juvenile female BALB/c mice, Food Chem. Toxicol. 97 (2016) 411–423.

[3] V. Reffatto, J.D. Rasinger, T.S. Carroll, T. Ganay, A.-K. Lundebye, I. Sekler, M. Hershfinkel, C. Hogstrand, Parallel in vivo and in vitro transcriptomics analysis reveals calcium and zinc signalling in the brain as sensitive targets of HBCD neurotoxicity, Arch. Toxicol. (2017) 1–15.

[4] European Food Safety Authority (EFSA), Scientific Opinion on Hexabromocyclododecanes (HBCDDs) in Food, EFSA Journal 9 (2011) 2296.

[5] C. Koch, T. Schmidt-Kötters, R. Rupp, B. Sures, Review of hexabromocyclododecane (HBCD) with a focus on legislation and recent publications concerning toxicokinetics and -dynamics, Environ. Pollut. 199 (2015) 26–34.

[6] L.T.M. Van der Ven, A. Verhoef, T. van de Kuil, W. Slob, P.E.G. Leonards, T.J. Visser, T. Hamers, M. Herlin, H. Hakansson, H. Olausson, A.H. Piersma, J.G. Vos, A 28-Day Oral Dose Toxicity Study Enhanced to Detect Endocrine Effects of Hexabromocyclododecane in Wistar Rats, Toxicol. Sci. 94 (2006) 281–292.

[7] F. Maranghi, R. Tassinari, G. Moracci, I. Altieri, J.D. Rasinger, T.S. Carroll, C. Hogstrand, A.-K. Lundebye, A. Mantovani, Dietary exposure of juvenile female mice to polyhalogenated seafood contaminants (HBCD, BDE-47, PCB-153, TCDD): comparative assessment of effects in potential target tissues, Food Chem. Toxicol. 56 (2013) 443–449.

[8] K. Ibhazehiebo, T. Iwasaki, N. Shimokawa, N. Koibuchi, 1,2,5,6,9,10-αHexabromocyclododecane (HBCD) impairs thyroid hormone-induced dendrite arborization of Purkinje cells and suppresses thyroid hormone receptor-mediated transcription, Cerebellum 10 (2011) 22–31.

[9] L.T.M. van der Ven, T. van de Kuil, P.E.G. Leonards, W. Slob, H. Lilienthal, S. Litens, M. Herlin, H. Håkansson, R.F. Cantón, M. van den Berg, T.J. Visser, H. van Loveren, J.G. Vos, A.H. Piersma, Endocrine effects of hexabromocyclododecane (HBCD) in a one-generation reproduction study in Wistar rats, Toxicol. Lett. 185 (2009) 51–62.

[10] H. Lilienthal, L.T.M. van der Ven, A.H. Piersma, J.G. Vos, Effects of the brominated flame retardant hexabromocyclododecane (HBCD) on dopamine-dependent behavior and brainstem auditory evoked potentials in a one-generation reproduction study in Wistar rats, Toxicol. Lett. 185 (2009) 63–72.

[11] E. Mariussen, F. Fonnum, The effect of brominated flame retardants on neurotransmitter uptake into rat brain synaptosomes and vesicles, Neurochem. Int. 43 (2003) 533–542.

[12] M.M.L. Dingemans, H.J. Heusinkveld, A. de Groot, A. Bergman, M. van den Berg, R.H.S. Westerink, Hexabromocyclododecane inhibits depolarization-induced increase in intracellular calcium levels and neurotransmitter release in PC12 cells, Toxicol. Sci. 107 (2009) 490–497.

[13] European Food Safety Authority (EFSA), Opinion of the Scientific Panel on Contaminants in the Food Chain on a request from the European Parliament related to the safety assessment of wild and farmed fish, EFSA Journal 3 (2005). doi:10.2903/j.efsa.2005.236.

[14] I.N. Pessah, G. Cherednichenko, P.J. Lein, Minding the calcium store: Ryanodine receptor activation as a convergent mechanism of PCB toxicity, Pharmacol. Ther. 125 (2010) 260–285.

[15] B. Wahlang, K.C. Falkner, B. Gregory, D. Ansert, D. Young, D.J. Conklin, A. Bhatnagar, C.J. McClain, M. Cave, Polychlorinated biphenyl 153 is a diet-dependent obesogen that worsens nonalcoholic fatty liver disease in male C57BL6/J mice, J. Nutr. Biochem. 24 (2013) 1587–1595.

[16] FAO/WHO, Safety evaluation of certain food additives and contaminants, Supplement 1: Non-dioxin-like polychlorinated biphenyls, World Health Organization, 2016. http://www.who.int/foodsafety/publications/food-additives-series-71-S1/en/ (accessed February 24, 2018).

[17] W. Yoshioka, R.E. Peterson, C. Tohyama, Molecular targets that link dioxin exposure to toxicity phenotypes, J. Steroid Biochem. Mol. Biol. 127 (2011) 96–101.

ACCEPTED MANUSCRIPT

[18] J.D. Rasinger, T.S. Carroll, A.K. Lundebye, C. Hogstrand, Cross-omics gene and protein expression profiling in juvenile female mice highlights disruption of calcium and zinc signalling in the brain following dietary exposure to CB-153, BDE-47, HBCD or TCDD, Toxicology 321 (2014) 1–12.
[19] G. Xu, Q. Zhou, C. Wan, Y. Wang, J. Liu, Y. Li, X. Nie, C. Cheng, G. Chen, 2,3,7,8-TCDD induces neurotoxicity and neuronal apoptosis in the rat brain cortex and PC12 cell line through the down-regulation of the Wnt/β-catenin signaling pathway, Neurotoxicology 37 (2013) 63–73.
[20] S.-Y. Kim, J.-H. Yang, Neurotoxic effects of 2,3,7,8-tetrachlorodibenzo-p-dioxin in cerebellar granule cells, Exp. Mol. Med. 37 (2005) 58–64.
[21] D.W. Nebert, A.L. Roe, M.Z. Dieter, W.A. Solis, Y. Yang, T.P. Dalton, Role of the aromatic hydrocarbon receptor and [Ah] gene battery in the oxidative stress response, cell cycle control, and apoptosis, Biochem. Pharmacol. 59 (1999) 65–85.
[22] D.W. Nebert, A. Puga, V. Vasiliou, Role of the Ah Receptor and the Dioxin-Inducible [Ah] Gene Battery in Toxicity, Cancer, and Signal Transduction, Ann NY Acad Sci. 685 (1993) 624–640.
[23] Y. Tian, Ah receptor and NF-kappaB interplay on the stage of epigenome, Biochem. Pharmacol. 77 (2009) 670–680.
[24] D.R. Boverhof, J.C. Kwekel, D.G. Humes, L.D. Burgoon, T.R. Zacharewski, Dioxin induces an estrogen-like, estrogen receptor-dependent gene expression response in the murine uterus, Mol. Pharmacol. 69 (2006) 1599–1606.
[25] L.E. Gray Jr, V.S. Wilson, T. Stoker, C. Lambright, J. Furr, N. Noriega, K. Howdeshell, G.T. Ankley, L. Guillette, Adverse effects of environmental antiandrogens and androgens on reproductive development in mammals, Int. J. Androl. 29 (2006) 96–104; discussion 105–8.
[26] European Commission, Opinion of the SCF on the Risk Assessment of Dioxins and Dioxin-like PCBs in Food, 2000. https://ec.europa.eu/food/sites/food/files/safety/docs/cs_contaminants_catalogue_dioxins_out90_en.pdf.
[27] European Food Safety Authority; Register of Questions. http://registerofquestions.efsa.europa.eu/raw-war/mandateLoader?mandate=M-2015-0011 (accessed February 24, 2018).
[28] F. Maranghi, A. Mantovani, Targeted toxicological testing to investigate the role of endocrine disrupters in puberty disorders, Reprod. Toxicol. 33 (2012) 290–296.
[29] E.A. Cohen Hubal, T. de Wet, L. Du Toit, M.P. Firestone, M. Ruchirawat, J. van Engelen, C. Vickers, Identifying important life stages for monitoring and assessing risks from exposures to environmental contaminants: results of a World Health Organization review, Regul. Toxicol. Pharmacol. 69 (2014) 113–124.
[30] L. Narciso, T. Catone, G. Aquilina, L. Attias, I. De Angelis, M.G. Iuliano, R. Tassinari, A. Mantovani, F. Maranghi, The juvenile toxicity study as a tool for a science-based risk assessment in the children population group, Reprod. Toxicol. (2017) doi:10.1016/j.reprotox.2017.06.188.
[31] K.P. Keenan, G.C. Ballam, K.A. Soper, P. Laroque, J.B. Coleman, R. Dixit, Diet, caloric restriction, and the rodent bioassay, Toxicol. Sci. 52 (1999) 24–34.
[32] S. Molon-Noblot, K.P. Keenan, J.B. Coleman, C.M. Hoe, P. Laroque, The effects of ad libitum overfeeding and moderate and marked dietary restriction on age-related spontaneous pancreatic islet pathology in Sprague-Dawley rats, Toxicol. Pathol. 29 (2001) 353–362.
[33] B. Martin, S. Ji, S. Maudsley, M.P. Mattson, "Control" laboratory rodents are metabolically morbid: why it matters, Proc. Natl. Acad. Sci. U. S. A. 107 (2010) 6127–6133.
[34] M. Haave, K.I. Folven, T. Carroll, C. Glover, E. Heegaard, T. Brattelid, C. Hogstrand, A.-K. Lundebye, Cerebral gene expression and neurobehavioural development after perinatal exposure to an environmentally relevant polybrominated diphenylether (BDE47), Cell Biol. Toxicol. 27 (2011) 343–361.
[35] A. Covaci, A.C. Gerecke, R.J. Law, S. Voorspoels, M. Kohler, N.V. Heeb, H. Leslie, C.R. Allchin, J. de Boer, Hexabromocyclododecanes (HBCDs) in the Environment and Humans: A Review, Environ. Sci. Technol. 40 (2006) 3679–3688.
[36] European Food Safety Authority (EFSA), Results of the monitoring of dioxin levels in food and feed, EFSA Journal 8 (2009) 1385.
[37] A. Shevchenko, M. Wilm, O. Vorm, M. Mann, Mass spectrometric sequencing of proteins silver-

ACCEPTED MANUSCRIPT

stained polyacrylamide gels, Anal. Chem. 68 (1996) 850–858.
[38] M. Wilm, A. Shevchenko, T. Houthaeve, S. Breit, L. Schweigerer, T. Fotsis, M. Mann, Femtomole sequencing of proteins from polyacrylamide gels by nano-electrospray mass spectrometry, Nature 379 (1996) 466–469.
[39] A. Keller, A.I. Nesvizhskii, E. Kolker, R. Aebersold, Empirical statistical model to estimate the accuracy of peptide identifications made by MS/MS and database search, Anal. Chem. 74 (2002) 5383–5392.
[40] A.I. Nesvizhskii, A. Keller, E. Kolker, R. Aebersold, A statistical model for identifying proteins by tandem mass spectrometry, Anal. Chem. 75 (2003) 4646–4658.
[41] Y. Ishihama, Y. Oda, T. Tabata, T. Sato, T. Nagasu, J. Rappsilber, M. Mann, Exponentially modified protein abundance index (emPAI) for estimation of absolute protein amount in proteomics by the number of sequenced peptides per protein, Mol. Cell. Proteomics. 4 (2005) 1265–1272.
[42] The Comparative Toxicogenomics Database | CTD, (n.d.). http://ctdbase.org/ (accessed March 13, 2018).
[43] O.J. Nøstbakken, H.T. Hove, A. Duinker, A.-K. Lundebye, M.H.G. Berntssen, R. Hannisdal, B.T. Lunestad, A. Maage, L. Madsen, B.E. Torstensen, K. Julshamn, Contaminant levels in Norwegian farmed Atlantic salmon (Salmo salar) in the 13-year period from 1999 to 2011, Environ. Int. 74 (2015) 274–280.
[44] A.-K. Lundebye, E.-J. Lock, J.D. Rasinger, O.J. Nøstbakken, R. Hannisdal, E. Karlsbakk, V. Wennevik, A.S. Madhun, L. Madsen, I.E. Graff, R. Ørnsrud, Lower levels of Persistent Organic Pollutants, metals and the marine omega 3-fatty acid DHA in farmed compared to wild Atlantic salmon (Salmo salar), Environ. Res. 155 (2017) 49–59.
[45] European Food Safety Authority (EFSA), Results of the monitoring of non dioxin-like PCBs in food and feed, EFSA Journal 8 (2010) doi:10.2903/j.efsa.2010.1701.
[46] R. Maronpot, Follicular Epithelial Cell Hypertrophy Induced by Chronic Oral Administration of 2,3,7,8-Tetrachlorodibenzo-p-Dioxin in Female Harlan Sprague–Dawley Rats - Toxicologic Pathology, Toxicologic Pathology. (2004). https://focusontoxpath.com/follicular-epithelial-cell-hypertrophy-induced-chronic-oral-administration-2378-tetrachlorodibenzo-p-dioxin-female-harlan-sprague-dawley-rats/ (accessed February 28, 2018).
[47] G.E. Krassas, K. Poppe, D. Glinoer, Thyroid function and human reproductive health, Endocr. Rev. 31 (2010) 702–755.
[48] H. Kohda, C. Sekiya, M. Kanai, Y. Yoshida, T. Uede, K. Kikuchi, M. Namiki, Flow cytometric and functional analysis of mononuclear cells infiltrating the liver in experimental autoimmune hepatitis, Clin. Exp. Immunol. 82 (1990) 473–478.
[49] S.A. Susin, E. Daugas, L. Ravagnan, K. Samejima, N. Zamzami, M. Loeffler, P. Costantini, K.F. Ferri, T. Irinopoulou, M.C. Prévost, G. Brothers, T.W. Mak, J. Penninger, W.C. Earnshaw, G. Kroemer, Two distinct pathways leading to nuclear apoptosis, J. Exp. Med. 192 (2000) 571–580.
[50] J.J. Heindel, B. Blumberg, M. Cave, R. Machtinger, A. Mantovani, M.A. Mendez, A. Nadal, P. Palanza, G. Panzica, R. Sargis, L.N. Vandenberg, F. Vom Saal, Metabolism disrupting chemicals and metabolic disorders, Reprod. Toxicol. 68 (2017) 3–33.
[51] G. Pearse, Histopathology of the Thymus, Toxicol. Pathol. 34 (2006) 515–547.
[52] K.D. Carpenter, C.A. Gray, T.M. Bryan, T.H. Welsh Jr, T.E. Spencer, Estrogen and antiestrogen effects on neonatal ovine uterine development, Biol. Reprod. 69 (2003) 708–717.
[53] T. Hamers, J.H. Kamstra, E. Sonneveld, A.J. Murk, M.H.A. Kester, P.L. Andersson, J. Legler, A. Brouwer, In vitro profiling of the endocrine-disrupting potency of brominated flame retardants, Toxicol. Sci. 92 (2006) 157–173.
[54] B.V. Krivoshiev, F. Dardenne, A. Covaci, R. Blust, S.J. Husson, Assessing in-vitro estrogenic effects of currently-used flame retardants, Toxicol. In Vitro. 33 (2016) 153–162.
[55] L.N. Vandenberg, T. Colborn, T.B. Hayes, J.J. Heindel, D.R. Jacobs Jr, D.-H. Lee, T. Shioda, A.M. Soto, F.S. vom Saal, W.V. Welshons, R.T. Zoeller, J.P. Myers, Hormones and endocrine-disrupting chemicals: low-dose effects and nonmonotonic dose responses, Endocr. Rev. 33 (2012) 378–455.
[56] European Food Safety Authority (EFSA), Modern methodologies and tools for human hazard assessment of chemicals, EFSA Journal 12 (2014) doi:10.2903/j.efsa.2014.3638.

ACCEPTED MANUSCRIPT

[57] J.D. Rasinger, A.-K. Lundebye, S.J. Penglase, S. Ellingsen, H. Amlund, Methylmercury Induced Neurotoxicity and the Influence of Selenium in the Brains of Adult Zebrafish (Danio rerio), Int. J. Mol. Sci. 18 (2017) 725.
[58] K. Winzer, C.J.F. Van Noorden, A. Köhler, Glucose-6-phosphate dehydrogenase: the key to sex-related xenobiotic toxicity in hepatocytes of European flounder (Platichthys flesus L.)?, Aquat. Toxicol. 56 (2002) 275–288.
[59] S. Nóbrega-Pereira, P.J. Fernandez-Marcos, T. Brioche, M.C. Gomez-Cabrera, A. Salvador-Pascual, J.M. Flores, J. Viña, M. Serrano, G6PD protects from oxidative damage and improves healthspan in mice, Nat. Commun. 7 (2016) 10894.
[60] W. Jeng, M.M. Loniewska, P.G. Wells, Brain glucose-6-phosphate dehydrogenase protects against endogenous oxidative DNA damage and neurodegeneration in aged mice, ACS Chem. Neurosci. 4 (2013) 1123–1132.
[61] Y.-P. Wang, L.-S. Zhou, Y.-Z. Zhao, S.-W. Wang, L.-L. Chen, L.-X. Liu, Z.-Q. Ling, F.-J. Hu, Y.-P. Sun, J.-Y. Zhang, C. Yang, Y. Yang, Y. Xiong, K.-L. Guan, D. Ye, Regulation of G6PD acetylation by SIRT2 and KAT9 modulates NADPH homeostasis and cell survival during oxidative stress, EMBO J. 33 (2014) 1304–1320.
[62] D. Harman, Aging: a theory based on free radical and radiation chemistry, J. Gerontol. 11 (1956) 298–300.
[63] T. Finkel, N.J. Holbrook, Oxidants, oxidative stress and the biology of ageing, Nature 408 (2000) 239–247.
[64] J. Legler, New insights into the endocrine disrupting effects of brominated flame retardants, Chemosphere 73 (2008) 216–222.
[65] D.K. Rawat, P. Hecker, M. Watanabe, S. Chettimada, R.J. Levy, T. Okada, J.G. Edwards, S.A. Gupte, Glucose-6-phosphate dehydrogenase and NADPH redox regulates cardiac myocyte L-type calcium channel activity and myocardial contractile function, PLoS One 7 (2012) e45365.
[66] F. Wang, H. Zhang, N. Geng, B. Zhang, X. Ren, J. Chen, New Insights into the Cytotoxic Mechanism of Hexabromocyclododecane from a Metabolomic Approach, Environ. Sci. Technol. 50 (2016) 3145–3153.
[67] E.R. Smith, K.L. Barker, Effects of estradiol and nicotinamide adenine dinucleotide phosphate on the rate of synthesis of uterine glucose 6-phosphate dehydrogenase, J. Biol. Chem. 249 (1974) 6541–6547.
[68] R.F. Kletzien, P.K. Harris, L.A. Foellmi, Glucose-6-phosphate dehydrogenase: a "housekeeping" enzyme subject to tissue-specific regulation by hormones, nutrients, and oxidant stress, FASEB J. 8 (1994) 174–181.
[69] R.J. Gonzales, S. Ansar, S.P. Duckles, D.N. Krause, Androgenic/estrogenic balance in the male rat cerebral circulation: metabolic enzymes and sex steroid receptors, J. Cereb. Blood Flow Metab. 27 (2007) 1841–1852.
[70] M.E.E. Jones, W.C. Boon, J. Proietto, E.R. Simpson, Of mice and men: the evolving phenotype of aromatase deficiency, Trends Endocrinol. Metab. 17 (2006) 55–64.
[71] Y. Gong, H. Xiao, C. Li, J. Bai, X. Cheng, M. Jin, B. Sun, Y. Lu, Y. Shao, H. Tian, Elevated t/e2 ratio is associated with an increased risk of cerebrovascular disease in elderly men, PLoS One 8 (2013) e61598.
[72] N. Benachour, S. Moslemi, H. Sipahutar, G.-E. Seralini, Cytotoxic effects and aromatase inhibition by xenobiotic endocrine disrupters alone and in combination, Toxicol. Appl. Pharmacol. 222 (2007) 129–140.
[73] S. Carreau, C. Delalande, D. Silandre, S. Bourguiba, S. Lambard, Aromatase and estrogen receptors in male reproduction, Mol. Cell. Endocrinol. 246 (2006) 65–68.
[74] R.A. Hill, S. Pompolo, M.E.E. Jones, E.R. Simpson, W.C. Boon, Estrogen deficiency leads to apoptosis in dopaminergic neurons in the medial preoptic area and arcuate nucleus of male mice, Mol. Cell. Neurosci. 27 (2004) 466–476.
[75] M.E.E. Jones, K.J. McInnes, W.C. Boon, E.R. Simpson, Estrogen and adiposity--utilizing models of aromatase deficiency to explore the relationship, J. Steroid Biochem. Mol. Biol. 106 (2007) 3–7.
[76] C.A. Cornil, On the role of brain aromatase in females: why are estrogens produced locally when they are available systemically?, J. Comp. Physiol. A Neuroethol. Sens. Neural Behav. Physiol. 204 (2018) 31–49.

ACCEPTED MANUSCRIPT

[77] A. Fucic, M. Gamulin, Z. Ferencic, J. Katic, M. Krayer von Krauss, A. Bartonova, D.F. Merlo, Environmental exposure to xenoestrogens and oestrogen related cancers: reproductive system, breast, lung, kidney, pancreas, and brain, Environ. Health 11 Suppl. 1 (2012) S8.

[78] E.C. Antunes-Fernandes, T.F.H. Bovee, F.E.J. Daamen, R.J. Helsdingen, M. van den Berg, M.B.M. van Duursen, Some OH-PCBs are more potent inhibitors of aromatase activity and (anti-) glucocorticoids than non-dioxin like (NDL)-PCBs and $MeSO_2$ -PCBs, Toxicol. Lett. 206 (2011) 158–165.

[79] M.G. Baldridge, G.T. Marks, R.G. Rawlins, R.J. Hutz, Very low-dose (femtomolar) 2,3,7,8-tetrachlorodibenzo-p-dioxin (TCDD) disrupts steroidogenic enzyme mRNAs and steroid secretion by human luteinizing granulosa cells, Reprod. Toxicol. 52 (2015) 57–61.

[80] J.R. Inglefield, W.R. Mundy, T.J. Shafer, Inositol 1,4,5-triphosphate receptor-sensitive Ca(2+) release, store-operated Ca(2+) entry, and cAMP responsive element binding protein phosphorylation in developing cortical cells following exposure to polychlorinated biphenyls, J. Pharmacol. Exp. Ther. 297 (2001) 762–773.

[81] D. Sul, H.-S. Kim, E.-K. Cho, M. Lee, H.S. Kim, W.-W. Jung, K.W. Hwang, S.-Y. Park, 2,3,7,8-TCDD neurotoxicity in neuroblastoma cells is caused by increased oxidative stress, intracellular calcium levels, and tau phosphorylation, Toxicology 255 (2009) 65–71.

[82] L.D. Brewer, A.L.S. Dowling, M.A. Curran-Rauhut, P.W. Landfield, N.M. Porter, E.M. Blalock, Estradiol reverses a calcium-related biomarker of brain aging in female rats, J. Neurosci. 29 (2009) 6058–6067.

[83] European Food Safety Authority (EFSA), Opinion of the Scientific Panel on contaminants in the food chain related to the presence of non dioxin-like polychlorinated biphenyls (PCB) in feed and food, EFSA Journal 3 (2005) doi:10.2903/j.efsa.2005.284.

[84] European Food Safety Authority (EFSA), Scientific Opinion on Polybrominated Diphenyl Ethers (PBDEs) in Food, (2011). http://www.efsa.europa.eu/en/efsajournal/doc/2156.pdf.

[85] European Food Safety Authority (EFSA), Update of the monitoring of levels of dioxins and PCBs in food and feed, EFSA Journal 10 (2012) doi:10.2903/j.efsa.2012.2832.

ACCEPTED MANUSCRIPT

ACCEPTED MANUSCRIPT

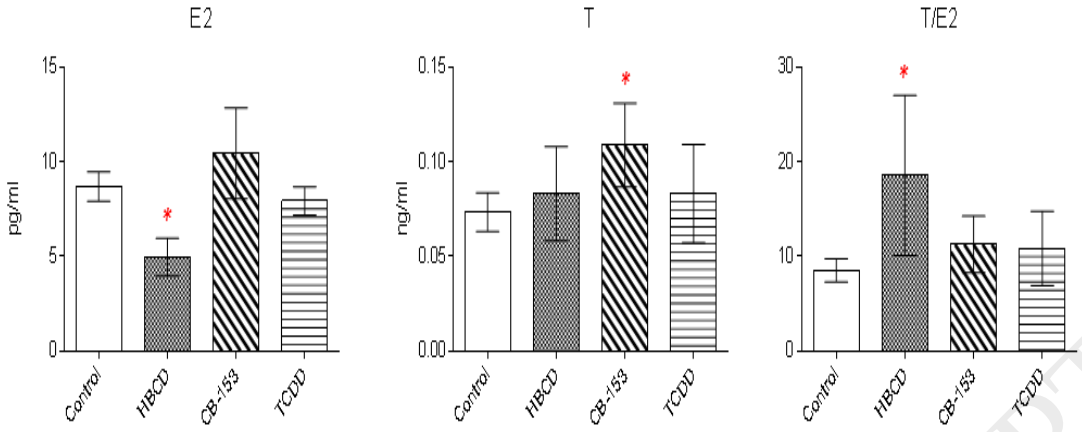

Figure 1. Testosterone (T) and 17β–oestradiol (E2) levels and T to E2 ratios (T/E2) in serum samples of juvenile female Balb/c mice after 28 days of repeated dietary exposure to HBCD (49.5 µg kg^{-1} bw^{-1} day^{-1}), CB-153 (1.35 µg kg^{-1} bw^{-1} day^{-1}) and TCDD (0.90 pg kg^{-1} bw^{-1} day^{-1}), respectively. Data are presented as mean ± standard deviation. Statistical significance (one-way ANOVA, n=10) is indicated by an asterisks sign (*).

ACCEPTED MANUSCRIPT

ACCEPTED MANUSCRIPT

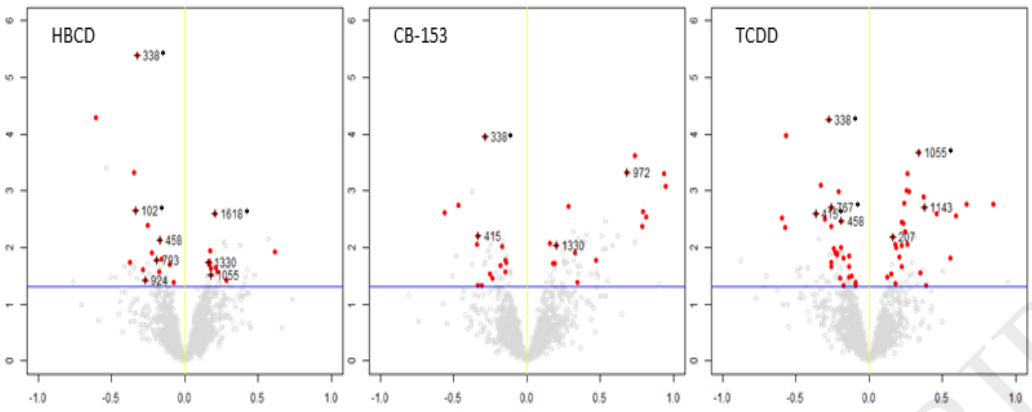

Figure 2. Proteomic responses detected in brains of BALB/c mice after 28 days of repeated dietary exposure exposed to HBCD (49.5 µg kg^{-1} bw^{-1} day^{-1}), CB-153 (1.35 µg kg^{-1} bw^{-1} day^{-1}) or TCDD (0.90 pg kg^{-1} bw^{-1} day^{-1}). Volcano plots show the calculated statistical significance on the y axis (expressed as −log10 p value) versus the estimated fold change on the x axis (expressed as ± log 2 fold change). Red dots represent differentially regulated proteins ($p < 0.05$); proteins differentially regulated at the $p<0.01$ level are highlighted with an asterisk (*). Red dots with black crosses represent the top ranked proteins, which have been identified successfully by LC–MS/MS. The numbers in the plots describe the unique protein spot identifiers. See Table S2A for further details on individual proteins.

ACCEPTED MANUSCRIPT

ACCEPTED MANUSCRIPT

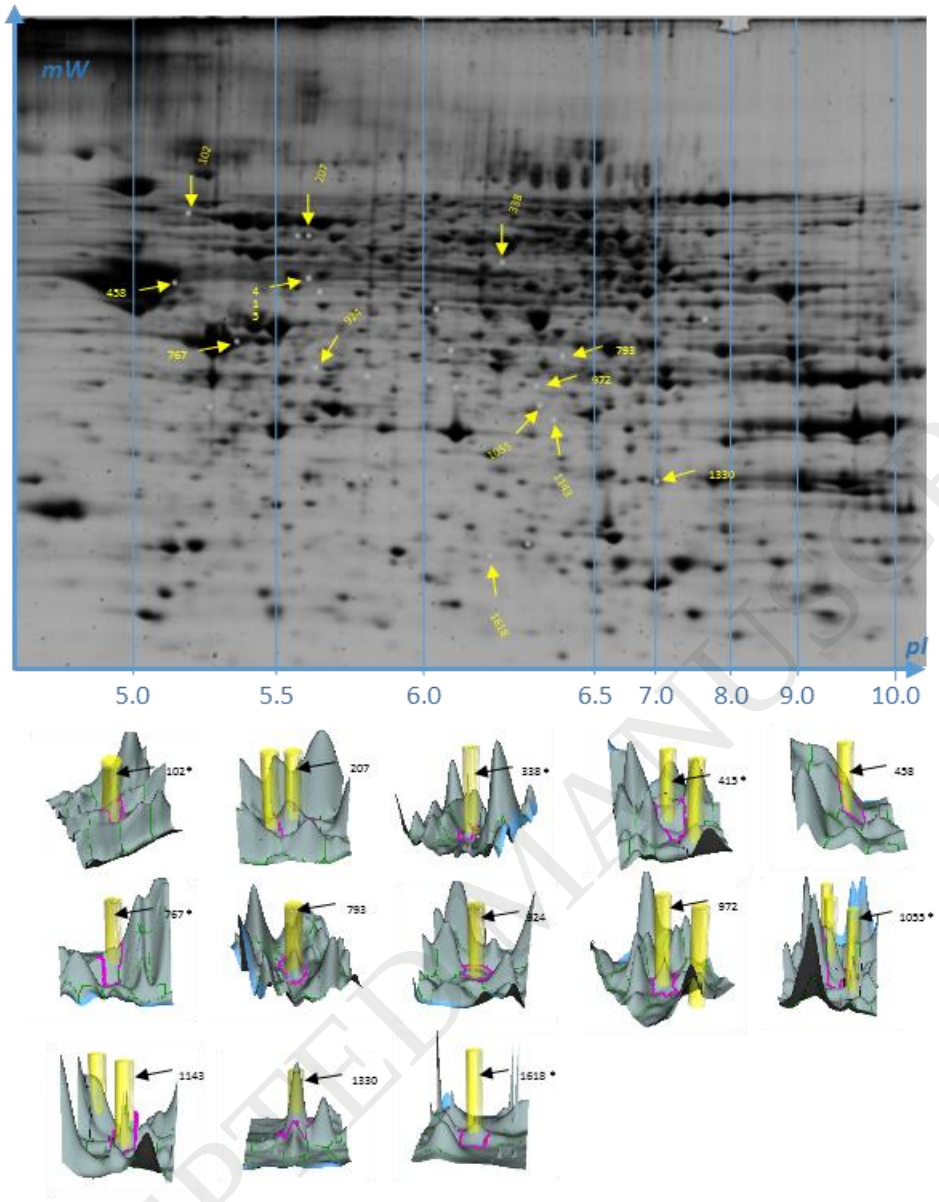

Figure 3. Preparative two-dimensional (2D) gel showing the picked and successfully identified significantly regulated ($p < 0.01$, ANOVA, n=18) proteins in brain of juvenile female BALB/c mice after 28 days of repeated dietary exposure exposed to HBCD (49.5 µg kg^{-1} bw-1 day^{-1} day^{-1}), CB-153 (1.35 µg kg^{-1} bw^{-1} day^{-1}) or TCDD (0.90 pg kg^{-1} bw^{-1} day^{-1}). Proteins differentially regulated at the $p<0.01$ level are highlighted with an asterisk (*). The numbers in the plot describe the unique difference in gel protein spot identifiers. The location of the spots relative to the x and y axes of the plot reflects the approximate isoelectric points and relative molecular weights, respectively of the detected protein spots. See Table S2B for further details on individual proteins.

ACCEPTED MANUSCRIPT

ACCEPTED MANUSCRIPT

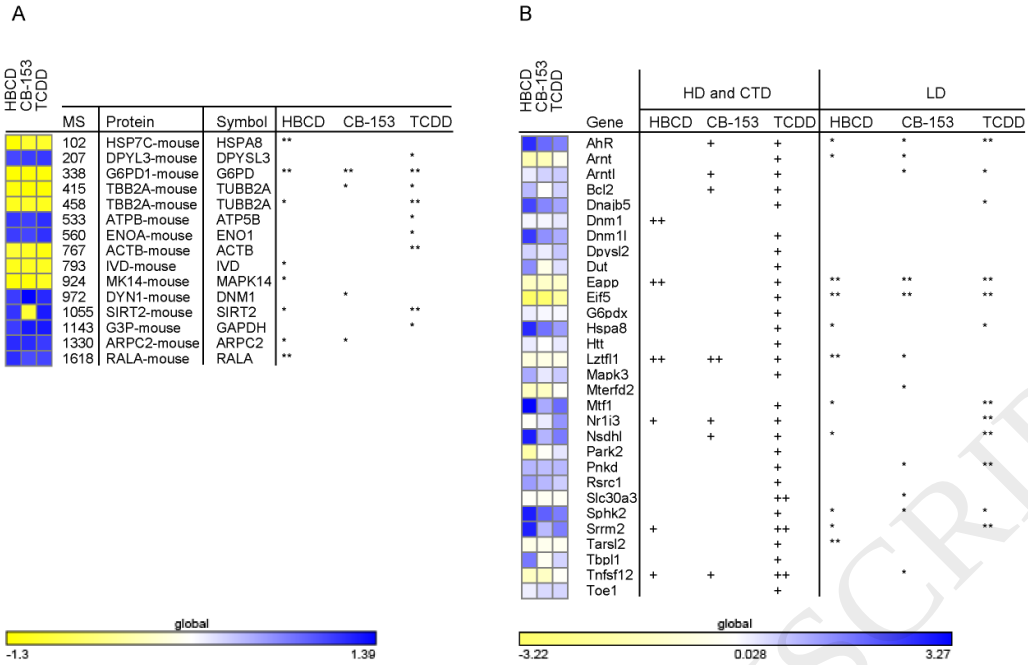

Figure 5. Heatmaps of differentially expressed proteins (**A**) and genes (**B**) in brain of juvenile female BALB/c mice after 28 days of repeated dietary exposure exposed to HBCD (49.5 µg kg^{-1} bw^{-1} day^{-1}), CB-153 (1.35 µg kg^{-1} bw^{-1} day^{-1}) or TCDD (0.90 pg kg^{-1} bw^{-1} day^{-1}). **A**: Protein names are provided alongside their unique 2D gel spot identifiers (MS) and gene symbol identifiers. Statistical significance is indicated by one asterisk sign (*) for the $p<0.05$ level and two asterisks signs (**) for the $p<0.01$ level. **B**: HD and CTD displays genes which according to literature were found to be differentially expressed after high dose exposure to high dose (HD) HBCD, CB-153 and TCDD. One plus (+) sign indicates listing in the Comparative Toxicogenomics Database (CTD) [42]; two plus signs (++) that these genes were also found to be differentially expressed in HD exposure to HBCD, CB-153 and TCDD [18]. LD displays genes which were found to be differentially expressed in the present study. Statistical significance is indicated by one asterisk sign (*) for the $p<0.05$ level and two asterisks signs (**) for the $p<0.01$ level. Yellow and blue boxes indicate up- and down regulation, respectively and the "global" bar at the bottom indicates the the upper and lower limits of the colour gradient. Additional data for all genes tested are presented in Table S3A. Blue and yellow boxes indicate up- and down regulation, respectively. Additional data for all proteins tested are presented in Table S3A.

ACCEPTED MANUSCRIPT

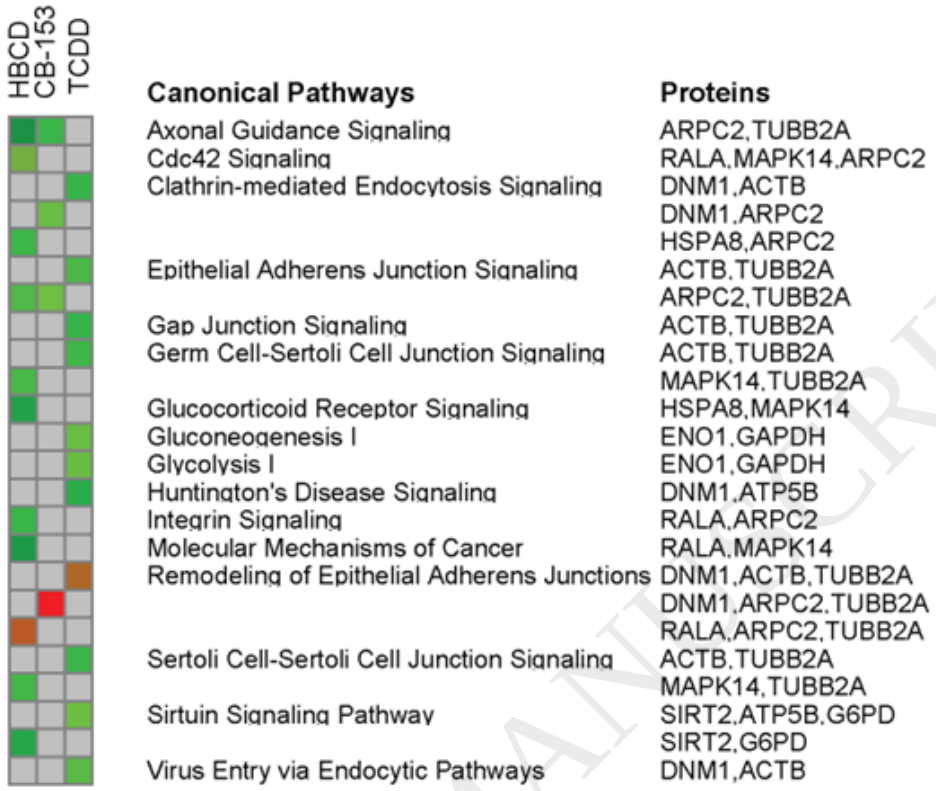

Figure 5. Ingenuity Pathway Analysis (IPA). Significantly regulated ($p < 0.05$) proteins in brain of juvenile female BALB/c mice after 28 days of repeated dietary exposure exposed to HBCD (49.5 µg kg^{-1} bw^{-1} day^{-1}), CB-153 (1.35 µg kg^{-1} bw^{-1} day^{-1}) or TCDD (0.90 pg kg^{-1} bw^{-1} day^{-1}) were grouped according to IPA "canonical pathways". In addition, over-representation of detected proteins in different "canonical pathways" was determined and is shown as a heatmap. Only selected pathways that were significantly ($p < 0.05$, Fisher's exact test) enriched in at least one of the exposure conditions are shown alongside their significance values expressed as scores (−log10 p-value). Scores above the cut-off (1.3) are displayed by a green to red colour gradient. Scores below the cut-off value are displayed as grey boxes. The full data-set including the proteins in each pathway is presented in Table S4A (proteins).

ACCEPTED MANUSCRIPT

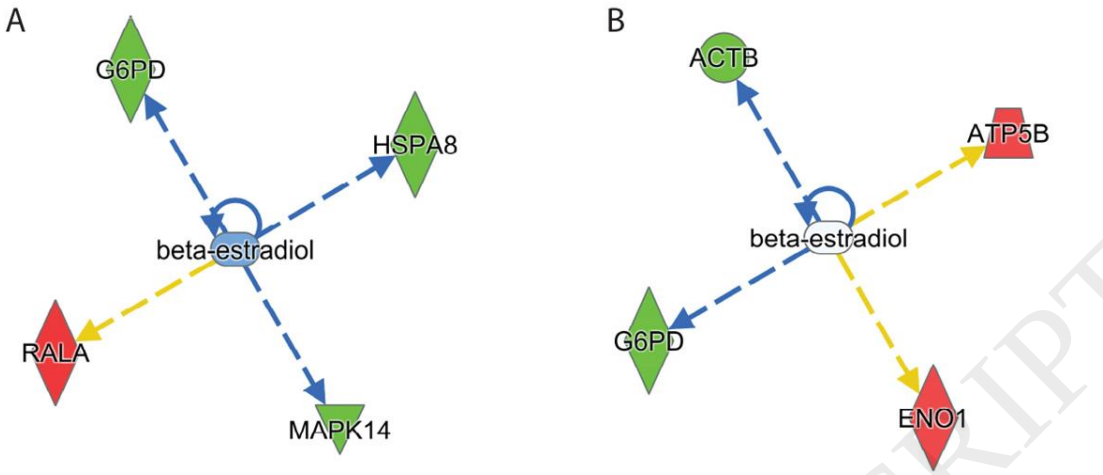

Figure 6. Ingenuity Pathway Analysis (IPA) of "upstream regulators". Significantly regulated ($p < 0.05$, ANOVA) proteins in brain of juvenile female BALB/c mice after 28 days of repeated dietary exposure exposed to HBCD (49.5 µg kg^{-1} bw^{-1} day^{-1}), CB-153 (1.35 µg kg^{-1} bw^{-1} day^{-1}) or TCDD (0.90 pg kg^{-1} bw^{-1} day^{-1}) were subjected to IPA. Changes observed in the brain of mice exposed to HBCD (**A**) and TCDD (**B**) are linked to decreased beta-estradiol levels. Activation (displayed in yellow) and inhibition (displayed in blue) of regulators and functions are based on IPA activation z-scores, which combine directional information encoded in the protein expression results with knowledge from the literature to make predictions about likely adverse outcome pathways. Up-regulated proteins are coloured red, down-regulated proteins are coloured green. The full data-sets of the upstream regulator analysis and the diseases and biological functions are presented in Table S4D.

ACCEPTED MANUSCRIPT

ACCEPTED MANUSCRIPT

Table 1. Histological evaluation of potential target tissues of persistent organic pollutant (POP) toxicity in juvenile female BALB/c mice after 28 days of repeated dietary exposure to HBCD (49.5 μg kg^{-1} bw-1 day^{-1}), CB-153 (1.35 μg kg^{-1} bw^{-1} day^{-1}) or TCDD (0.90 pg kg^{-1} bw^{-1} day^{-1}), respectively. Statistically significant differences in the categorical data obtained were elucidated by two tailed Fisher's Exact Tests. Significant effects at the $p<0.05$ levels, are indicated by an asterisks sign (*).

Tissue	Observations	Group			
		Control	HBCD	CB-153	TCDD
Thyroid	Desquamation into follicular lumen	0/7	3/7	2/7	0/7
	Foaming colloid	1/7	2/7	4/7	3/7
Uterus	Irregular multistratification of the luminal epithelium	1/8	2/7	3/9	4/6
	Reduction in endometrial glands density	0/8	4/7*	2/9	2/6
Liver	Marked vacuolization in hepatocytes	0/10	5/8*	1/8	2/8
	Lymphocytic infiltration	0/10	6/8*	4/8*	4/8 *
	Hyperaemic vessels	0/10	6/8*	0/8	1/8
	Picnotic nucleus	0/10	2/8	2/8	2/8
Adrenals	Thickness external capsule	2/10	3/7	2/9	3/8
Thymus	Hassal's bodies	2/10	5/10	4/10	2/10
	Cortical invasivity	2/10	2/10	4/10	2/10
	Minerals	2/10	5/10	0/10	6/10
	Stress	0/10	5/10*	7/10*	0/10
Spleen	Lymphocyte hyperplasia	4/10	5/10	2/10	6/10
	Infiltration in red pulp and periarteriolar zones (PALS)	0/10	0/10	2/10	0/10
Brain	Eosinophilic cells in the cortex	2/10	3/8	4/9	4/10
	Eosinophilic cells in the thalamus	3/10	2/8	4/9	0/10
	Condensed cells in the hypothalamus	0/10	1/8	0/9	0/10

ACCEPTED MANUSCRIPT

Table 2. Histomorphological evaluation of potential target tissues of persistent organic pollutant (POP) toxicity in juvenile female BALB/c mice after 28 days of repeated dietary exposure to HBCD (49.5 µg kg^{-1} bw^{-1} day^{-1}), CB-153 (1.35 µg kg^{-1} bw^{-1} day^{-1}) or TCDD (0.90 pg kg^{-1} bw^{-1} day^{-1}), respectively. Statistically significant differences in the categorical data obtained were elucidated by two tailed Mann-Whitney U Test. Significant effects at the $p<0.05$ levels, are indicated by an asterisks sign (*).

Tissue	Measures	Group			
		Control	HBCD	CB-153	TCDD
Thyroid		n=5	n=5	n=5	n=5
	Ratio between follicle and colloid areas	1.41 ± 0.07	1.46 ± 0.10	1.51 ± 0.13	1.52 ± 0.09
	Follicle area (μm^2)	2402 ± 500	1691 ± 608	1830 ± 754	1435 ± 256
	Colloid area (μm^2)	1718 ± 403	1190 ± 535	1251 ± 590	953 ± 202
	Ratio of follicular epithelium areas and number of nuclei	2.14 ± 0.09	2.57 ± 0.27*	2.91 ± 0.74*	2.66 ± 0.41
Uterus		n=8	n=7	n=8	n=6
	Ratio between area of endometrium and myometrium	4.07 ± 1.18	4,82 ± 1.14	4,30 ± 1.17	3,61 ± 1.56
Adrenals		n = 8	n=5	n=5	n=4
	Ratio between cortex and medulla areas	5.50 ± 1.59	7,44 ± 1.49	7,91 ± 3.96	5,65 ± 2.21
Thymus		n=6	n=8	n=7	n=7
	Ratio between cortex and medulla areas	2.55 ± 0.77	2,64 ± 1.18	3,75 ± 1.88	3,39 ± 0.91
Spleen		n=8	n=10	n=10	n=7
	Ratio between red pulp and white pulp areas	2.54 ± 0.85	1,00 ± 0.30	1,40 ± 0.34	3,32 ± 1.75

ACCEPTED MANUSCRIPT